Nuclear transparency from quasielastic $A(e,e'p)$ reactions up to $Q^2=8.1$ (GeV/c)^2

K. Garrow,[18] D. McKee,[13] A. Ahmidouch,[14] C. S. Armstrong,[18] J. Arrington,[2] R. Asaturyan,[22] S. Avery,[7] O. K. Baker,[7,18] D. H. Beck,[8] H. P. Blok,[20] C. W. Bochna,[8] W. Boeglin,[4,18] P. Bosted,[1,*] M. Bouwhuis,[8] H. Breuer,[9] D. S. Brown,[9] A. Bruell,[10] R. D. Carlini,[18] N. S. Chant,[9] A. Cochran,[7] L. Cole,[7] S. Danagoulian,[14] D. B. Day,[19] J. Dunne,[12] D. Dutta,[10] R. Ent,[18] H. C. Fenker,[18] B. Fox,[3] L. Gan,[7] D. Gaskell,[2,16] A. Gasparian,[7] H. Gao,[10] D. F. Geesaman,[2] R. Gilman,[17,18] P. L. J. Guèye,[7] M. Harvey,[7] R. J. Holt,[8,†] X. Jiang,[17] C. E. Keppel,[7,18] E. Kinney,[3] Y. Liang,[1,7] W. Lorenzon,[11] A. Lung,[18] D. J. Mack,[18] P. Markowitz,[4,18] J. W. Martin,[10] K. McIlhany,[10] D. Meekins,[5,‡] M. A. Miller,[8] R. G. Milner,[10] J. H. Mitchell,[18] H. Mkrtchyan,[22] B. A. Mueller,[2] A. Nathan,[8] G. Niculescu,[15] I. Niculescu,[6] T. G. O'Neill,[2] V. Papavassiliou,[13,18] S. Pate,[13,18] R. B. Piercey,[12] D. Potterveld,[2] R. D. Ransome,[17] J. Reinhold,[4,18] E. Rollinde,[18,21] P. Roos,[9] A. J. Sarty,[5,§] R. Sawafta,[14] E. C. Schulte,[8] E. Segbefia,[7] C. Smith,[19] S. Stepanyan,[22] S. Strauch,[17] V. Tadevosyan,[22] L. Tang,[7,18] R. Tieulent,[9,18] A. Uzzle,[7] W. F. Vulcan,[18] S. A. Wood,[18] F. Xiong,[10] L. Yuan,[7] M. Zeier,[19] B. Zihlmann,[19] and V. Ziskin[10]

[1]*American University, Washington, D.C. 20016*
[2]*Argonne National Laboratory, Argonne, Illinois 60439*
[3]*University of Colorado, Boulder, Colorado 80309*
[4]*Florida International University, University Park, Florida 33199*
[5]*Florida State University, Tallahassee, Florida 32306*
[6]*The George Washington University, Washington, D.C. 20052*
[7]*Hampton University, Hampton, Virginia 23668*
[8]*University of Illinois, Champaign-Urbana, Illinois 61801*
[9]*University of Maryland, College Park, Maryland 20742*
[10]*Massachusetts Institute of Technology, Cambridge, Massachusetts 02139*
[11]*University of Michigan, Ann Arbor, Michigan 48109*
[12]*Mississippi State University, Mississippi State, Mississippi 39762*
[13]*New Mexico State University, Las Cruces, New Mexico 88003*
[14]*North Carolina A & T State University, Greensboro, North Carolina 27411*
[15]*Ohio University, Athens, Ohio 45071*
[16]*Oregon State University, Corvallis, Oregon 97331*
[17]*Rutgers University, New Brunswick, New Jersey 08903*
[18]*Thomas Jefferson National Accelerator Facility, Newport News, Virginia 23606*
[19]*University of Virginia, Charlottesville, Virginia 22901*
[20]*Vrije Universiteit, 1081 HV Amsterdam, The Netherlands*
[21]*College of William and Mary, Williamsburg, Virginia 23187*
[22]*Yerevan Physics Institute, 375036 Yerevan, Armenia*

(Received 29 August 2001; published 25 October 2002)

The quasielastic $(e,e'p)$ reaction was studied on targets of deuterium, carbon, and iron up to a value of momentum transfer Q^2 of 8.1 (GeV/c)^2. A nuclear transparency was determined by comparing the data to calculations in the plane-wave impulse approximation. The dependence of the nuclear transparency on Q^2 and the mass number A was investigated in a search for the onset of the color transparency phenomenon. We find no evidence for the onset of color transparency within our range of Q^2. A fit to the world's nuclear transparency data reflects the energy dependence of the free-proton–nucleon cross section.

DOI: 10.1103/PhysRevC.66.044613 PACS number(s): 25.30.Fj, 24.85.+p

I. INTRODUCTION

The concept of color transparency (CT) was introduced two decades ago by Mueller and Brodsky [1], and since has stimulated great experimental and theoretical interest. CT is an effect of QCD, related to the presence of nonabelian color degrees of freedom underlying strongly interacting matter. CT has its most unique manifestation in $A(p,2p)$ or $A(e,e'p)$ experiments at high energies. The basic idea is that, under the right conditions, three quarks, each of which would normally interact very strongly with nuclear matter, could form an object that passes undisturbed through the nuclear medium. A similar phenomenon occurs in QED, where an e^+e^- pair of small size has a small cross section determined by its electric dipole moment [2]. In QCD, a $q\bar{q}$ or qqq system can act as an analogous small color dipole moment.

*Present address: University of Massachusetts, Amherst, MA 01003.
†Present address: Argonne National Laboratory, Argonne, IL 60439.
‡Present address: TJNAF, Newport News, VA 23606.
§Present address: St. Mary's University, Halifax, NS, Canada B3H 3C3.

CT was first discussed in the context of perturbative QCD. Later work [3] indicates that this phenomenon also occurs in a wide variety of model calculations with nonperturbative reaction mechanisms. In general, the existence of CT requires that high momentum transfer scattering takes place via selection of amplitudes in the initial and final state hadrons characterized by a small transverse size. Second, this small object should be ''color neutral'' outside of this small radius in order not to radiate gluons. Finally, this compact size must be maintained for some distance in traversing the nuclear medium. Unambiguous observation of CT would provide new means to study the strong interaction in nuclei.

Several measurements of the transparency of the nuclear medium to high energy protons in quasielastic $A(p,2p)$ and $A(e,e'p)$ reactions have been carried out over the last decade. The nuclear transparency measured in $A(p,2p)$ at Brookhaven [4] has shown a rise consistent with CT for $Q^2 \simeq 3$–8 $(\mathrm{GeV}/c)^2$, but decreases at higher momentum transfer. At the time, questions were raised about the interpretation of this data, as only one of the two final-state protons was momentum analyzed, and the exclusivity of the reaction could not be guaranteed. A more recent experiment [5], completely reconstructing the final state of the $A(p,2p)$ reaction, confirms the validity of the earlier Brookhaven experiment. Two explanations for the surprising behavior were given: Ralston and Pire [6] proposed that the interference between short and long distance amplitudes in the free p-p cross section was responsible for these energy oscillations, where the nuclear medium acts as a filter for the long distance amplitudes. Brodsky and De Teramond [7] argued that the unexpected decrease could be related to the crossing of the open-charm threshold.

The NE-18 $A(e,e'p)$ measurements at SLAC [8,9] yielded distributions in missing energy and momentum completely consistent with conventional nuclear physics predictions. The extracted transparencies exclude sizable CT effects up to $Q^2 = 6.8$ $(\mathrm{GeV}/c)^2$, in contrast to the $A(p,2p)$ results [4]. The measurements ruled out several models predicting an early, rapid onset of CT, but could not exclude models predicting a slow onset of CT. The proposed explanation of Ralston and Pire [6], that the nuclear medium A eliminates the long distance amplitudes in the $A(p,2p)$ case, might resolve the apparent discrepancy between the $A(e,e'p)$ and $A(p,2p)$ results. Still, questions remain with the recent claim that the nuclear transparencies at $Q^2 \simeq 8$ $(\mathrm{GeV}/c)^2$ in $A(p,2p)$ experiments deviate from Glauber predictions [5].

Intuitively, one expects an earlier onset of CT for meson production than for hard proton scattering, as it is much more probable to produce a small transverse size in a $q\bar{q}$ system than in a three quark system. By contrast, microscopic calculations for meson production from nuclei may be on less solid footing than in the comparable $A(e,e'p)$ case. Nuclear transparencies in exclusive incoherent ρ^0 meson production from nuclei have been measured in several experiments. At Fermilab [10], increases in the nuclear transparencies have been observed as the virtuality of the photon increases, as expected from CT. Inclusion of CERN data on similar nuclear transparencies, at higher Q^2, however, make the effect less significant [11]. In addition, for such reactions one has to distinguish coherence length from formation length effects. The coherence length is the distance at which the virtual photon fluctuates into a $q\bar{q}$ pair. The formation length is the distance traveled by the small size $q\bar{q}$ pair before evolving to the normal ρ meson size. Formation lengths are the governing scales to look for the CT effects. Evidence for strong coherence length effects has recently been reported by the HERMES experiment at DESY [12]. It should be noted that for the Fermilab experiment formation lengths are only a factor of approximately 2–3 larger than coherence lengths.

Recent support for CT comes from the coherent diffractive dissociation of 500 GeV/c negative pions into dijets [13]. Such a dijet production reaction is not an exclusive reaction, and may thus differ fundamentally from other searches for CT. The inferred Q^2 for this reaction was larger than 7 $(\mathrm{GeV}/c)^2$. The A dependence of the data was fit assuming $\sigma \propto A^{\alpha}$ for three k_t bins, with k_t the jet transverse momentum. For $1.25 < k_t < 1.5$ GeV/c, $1.5 < k_t < 2.0$ GeV/c, and $2.0 < k_t < 2.5$ GeV/c ($Q^2 \geq 4k_t^2$) the alpha values were determined to be $\alpha = 1.64^{+0.06}_{-0.12}$, $\alpha = 1.52 \pm 0.12$, and $\alpha = 1.55 \pm 0.16$, respectively. This is far larger than the $\sigma \propto A^{0.7}$ dependence typically found in inclusive π-nucleus scattering, whereas the theoretical [14] CT values were predicted to be $\alpha = 1.25$, 1.45, and 1.60, respectively. These dijet data, however, do not inform about the kinematic onset of CT. To date, none of the mentioned measurements provides direct information on the onset of CT.

Quasielastic $A(e,e'p)$ reactions have several advantages to offer in searching for CT effects. The fundamental e-p scattering cross section is smoothly varying and accurately known; compared to the $A(p,2p)$ reaction one has less sensitivity to the unknown large momentum components of the nuclear wave function [15]; energy resolutions are sufficient to guarantee the exclusivity of the reaction; and, one does not have to distinguish coherence length effects. The purpose of the present experiment was to measure the nuclear transparency in the $A(e,e'p)$ reaction with greatly improved statistics and systematic uncertainties compared to the NE-18 experiment [8,9], and to increase the Q^2 range in order to search for the onset of CT. The precision of the presented data, in addition to the reliability of conventional nuclear transparency calculations for the $A(e,e'p)$ reaction, allows for a conclusive test of such an onset.

II. EXPERIMENT AND DATA ANALYSIS

The experiment was performed at the Thomas Jefferson National Accelerator Facility (TJNAF). Beam energies of 3.059, 4.463, and 5.560 GeV were used for the Q^2 values of 3.3, 6.1, and 8.1 $(\mathrm{GeV}/c)^2$, respectively. The electron beam impinged on either a cryogenic target system, consisting of 4.5 cm long liquid hydrogen and deuterium targets, cooled to 19 K and 22 K, respectively, or a solid target system, which incorporated a solid ^{12}C target of 3% radiation length and solid ^{56}Fe targets of 3% and 6% radiation length. The target thickness uncertainty is estimated to be 0.3% for the solid

TABLE I. Kinematics for the present experiment. The quasifree angles are indicated in boldface.

Average $T_{p'}$ (MeV)	Electron energy (GeV)	Q^2 $(\mathrm{GeV}/c)^2$	Electron θ_{LAB} (deg.)	Proton θ_{LAB} (deg)
1760	3.059	3.3	54.00	19.78, 22.30, **24.81**, 27.28, 29.78
3263	4.463	6.1	64.65	**15.33**
4293	5.560	8.1	64.65	**12.84**

targets, and 0.5% for the liquid targets.

An aluminum dummy target, consisting of two 0.99 mm Al targets separated by 4.5 cm, was suspended from the cryogenic target system in order to subtract the 0.13 mm Al window contributions to the cryogenic targets. Beam currents ranged from 30 to 60 μA depending on the target used. The beam current was measured by a system of beam current monitors along with a parametric current transformer for absolute calibration. The error in the absolute calibration due to noise was less than 0.2 μA. Thus, the error in the accumulated beam charge is less than 1%. The High Momentum Spectrometer (HMS) and Short Orbit Spectrometer (SOS) were used to detect the knocked-out proton and scattered electron, respectively. The spectrometers and their detection packages are described in Ref. [16]. The momentum acceptance ($\Delta p/p$) utilized in the HMS was $\pm 8\%$, and in the SOS $\pm 15\%$. The various kinematics are given in Table I.

In addition to the coincident $A(e,e'p)$ data, for all kinematics a subset of single events was recorded with a statistical accuracy of much better than 1%. This enabled monitoring the product of detector efficiencies, accumulated charge and target density effects on a run-to-run basis. Since the target density of the cryogenic targets is influenced by heating effects due to the incident electron beam, a correction was applied. This correction was $(2.0\pm 0.4)\%$ for the highest beam current (60 μA).

Prior to the start of the $A(e,e'p)$ experiment, $^1\mathrm{H}(e,e')$ elastic electron-proton events were recorded in both spectrometers at a beam energy of 2.056 GeV. Both spectrometers measured a fixed scattered electron momentum of 1.350 GeV/c, while the spectrometer angles were varied from 32.9° to 42.9° to scan the elastically scattered electrons across the spectrometer momentum acceptance. The known hydrogen cross section [17] was then used to check the spectrometers for both normalization and acceptance problems. The measured and simulated HMS data agreed to better than 2% for the entire momentum acceptance used in the data analysis. The SOS acceptance, however, showed a complicated correlation among the vertex position (y_{target}), the angle of the scattered electron (y'_{target}), and the momentum deviation of the scattered electron ($\delta p/p$). The latter two are defined with respect to the nominal spectrometer angle and momentum, respectively. Simulations showed that such correlated effects become important when using a target with an effective target length (i.e., the target length as viewed by the spectrometer) larger than about 2.5 cm. For elastic scattering y'_{target} and $\delta p/p$ are correlated, and we found normalization problems at large $\pm y_{target}$ and large $\pm y'_{target}$. The $\mathrm{H}(e,e')$ calibration runs approached a normalization consistent with the expectations based upon the world $\mathrm{H}(e,e')$ cross sections [17], however, when a small y_{target} cut was used.

In the actual $A(e,e'p)$ data taking the SOS was positioned at far larger scattering angles (see Table I), to obtain the highest possible Q^2, and was thus even more susceptible to this acceptance problem. Although we do believe that we have understood the acceptance problem, we took the simple solution of normalizing the $\mathrm{D}(e,e'p)$ data to the $\mathrm{H}(e,e'p)$ results. Any lack of understanding of the extended target acceptance cancels in the ratio of yields of two similar, extended targets. It was, indeed, verified that the ratio of the deuterium and hydrogen yields, within statistics, does not depend on the cut on y_{target}. It should be noted that the measurements on the almost pointlike solid targets are not affected by the mentioned acceptance problem.

For the $A(e,e'p)$ results, the yields were corrected for proton absorption in the target and through the various components of the spectrometer. This correction varied from 5 to 6.5% depending on the target used. The correction could be partially checked by comparing elastic $^1\mathrm{H}(e,e')$ and $^1\mathrm{H}(e,e'p)$ rates. The uncertainty in the correction is estimated to be 1%.

Coincident detection of the recoil electron and ejected proton momentum enabled the determination of the energy transfer, $\nu = E_e - E_{e'}$, where E_e is the electron beam energy and $E_{e'}$ is the energy of the detected electron, and the missing energy $E_m = \nu - T_{p'} - T_{A-1}$, where $T_{p'}$ and T_{A-1} are the kinetic energies of the final-state proton and $A-1$ recoil nucleus, respectively. Also, the missing momentum $\vec{p}_m = \vec{p}_{p'} - \vec{q}$, where $\vec{p}_{p'}$ and $\vec{q}$ are the momentum of the detected proton and the three-momentum transfer in the interaction, can be computed. The missing energy E_m is equal to the separation energy E_s needed to remove the nucleon from a particular state within the nucleus. Assuming the plane-wave impulse approximation (PWIA) to be valid, the missing momentum $\vec{p}_m$ is equal to the initial momentum of the proton within the nucleus. In a nonrelativistic PWIA formalism, the cross section can be written in a factorized form as

$$\frac{d^6\sigma}{dE_{e'}d\Omega_{e'}dE_{p'}d\Omega_{p'}} = K\sigma_{ep}S(E_m,\vec{p}_m), \tag{1}$$

where $dE_{e'}, d\Omega_{e'}, dE_{p'}$, and $d\Omega_{p'}$ are the phase space factors of the electron and proton, $K = |\vec{p}_{p'}|E_{p'}$ is a known kinematical factor, and σ_{ep} is the off-shell electron-proton cross section. The choice of the off-shell cross section [18] is

set by choosing a prescription to apply momentum and energy conservation at the $\gamma_v p$ vertex. Here, γ_v is the virtual photon with energy ν and three-momentum $\vec{q}$, and p represents an off-shell proton, with initial momentum $\vec{p_p}$ and separation energy E_m. The spectral function $S(E_m,\vec{p}_m)$ is defined as the joint probability of finding a proton of momentum $\vec{p}_m$ and separation energy E_m within the nucleus. This function contains the nuclear structure information for a given nucleus.

The definition of the transparency ratio is the same as in the early, pioneering $A(e,e'p)$ CT experiment [8,9], that is, the ratio of the cross section measured in a nuclear target to the cross section for $(e,e'p)$ scattering in PWIA. Numerically this ratio can be written as

$$T(Q^2)=\frac{\int_V d^3p_m dE_m Y_{exp}(E_m,\vec{p}_m)}{\int_V d^3p_m dE_m Y_{PWIA}(E_m,\vec{p}_m)}, \qquad (2)$$

where the integral is over the phase space V defined by the cuts $E_m<80$ MeV and $|\vec{p}_m|<300$ MeV/c, $Y_{exp}(E_m,\vec{p}_m)$ and $Y_{PWIA}(E_m,\vec{p}_m)$ are the corresponding experimental and simulation yields. The E_m cut prevents inelastic contributions above pion production threshold.

The off-shell prescription σ_1^{cc} of Ref. [18] was used for the evaluation of σ_{ep} in Eq. (1). The measured nuclear transparencies are hardly sensitive to the inclusion of such off-shell effects, — using an on-shell form changes T by less than 1%. The spectral functions used as input to the simulation are the same as in Refs. [8,9]. The distribution of events in E_m (describing knockout from particular orbits) is characterized by Lorentzian energy profiles to account for the spreading width of the one-hole states. The momentum distributions are calculated using a Woods-Saxon nuclear potential with shell-dependent parameters. The Lorentzian and Woods-Saxon parameters are determined from fits to spectral functions extracted from previous $A(e,e'p)$ experiments [19]. Descriptions of the deepest-lying shells of Fe were taken from a Hartree-Fock calculation [20] since data on these shells are inconclusive.

These spectral functions are generated with the assumption of an independent-particle model, which is known to overestimate the experimental yield from a given shell model configuration, as defined via $(E_m,|\vec{p}_m|)$ limits. Nucleon-nucleon correlations are not contained in such a formalism and are known to move independent-particle model yields to higher excitation energies. In order to account for this, a so-called correlation correction was applied. The correlation corrections for the kinematical cuts applied to the data, $E_m<80$ MeV and $|\vec{p}_m|<300$ MeV/c, were 1.11 (1.22) for ^{12}C (^{56}Fe); these corrections have uncertainties estimated to be 0.03 (0.06). These correlation corrections have been previously determined from ^{12}C and ^{16}O [21] spectral functions that include the effects of correlations. For Fe, a correlated nuclear matter spectral function corrected for finite nucleus

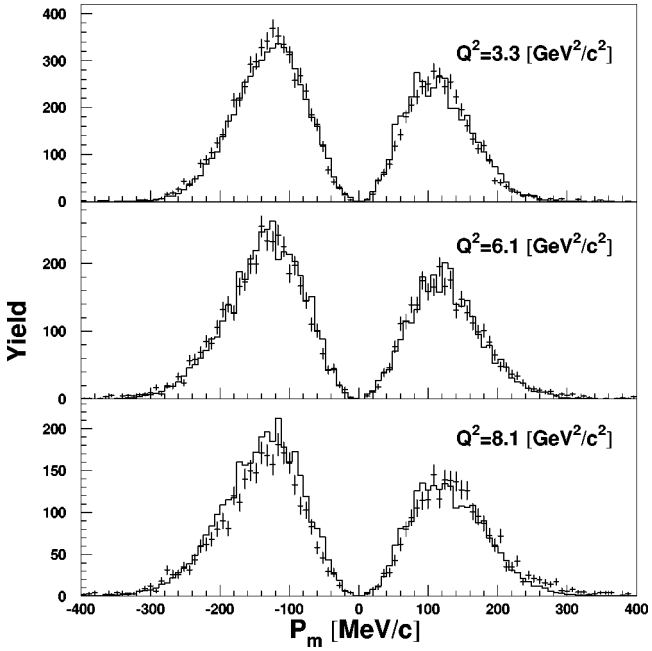

FIG. 1. Experimental yield (pluses) as a function of missing momentum for the ^{12}C$(e,e'p)$ reaction, with the hadron spectrometer positioned at the quasifree angle, compared to simulated yields (histogram), at $Q^2=3.3$, 6.1, and 8.1 (GeV/c)^2. The data are integrated over a missing energy region up to 80 MeV. Positive (negative) missing momentum is defined as a proton angle larger (smaller) than the momentum transfer angle.

effects [22] was used to estimate this correction factor. These correlation corrections would correspond to spectroscopic factors that are higher than what has been determined from lower Q^2 $A(e,e'p)$ data, by typically 20% [or $1-2\sigma$] [23,24]. This is an unresolved issue [25]. One cannot determine spectroscopic factors independently from nuclear transparencies. Here, we use the mentioned correlation corrections for consistency with previous nuclear transparency data [8,9,16].

The measured ^{12}C$(e,e'p)$ yields, as function of missing momentum, and the predictions from the simulation are shown in Fig. 1. The requirement that $E_m<80$ MeV was applied to both data and Monte Carlo distributions. Good agreement between the momentum distributions is observed for all Q^2 points measured. Similarly, we obtain good agreement between the experimental and simulated ^{12}C$(e,e'p)$ yields as function of missing energy. This is illustrated for the $Q^2=6.1$ (GeV/c)^2 kinematics in Fig. 2. Radiative corrections are applied as described in Ref. [26]. Their net effect, for these kinematics, is a renormalization of the integrated yield, up to $E_m=80$ MeV, by 36%. For the ^{56}Fe$(e,e'p)$ case good agreement is found for the momentum distributions, but discrepancies between data and simulations can be observed in the missing energy distributions.

For the lowest Q^2 point of 3.3 (GeV/c)^2 the Fermi cone was mapped by varying the angle of the proton spectrometer about the quasifree angle. The upper panel of Fig. 3 shows the normalized yield for the various angles about the quasifree angle for the ^{12}C and ^{56}Fe targets. The solid symbols

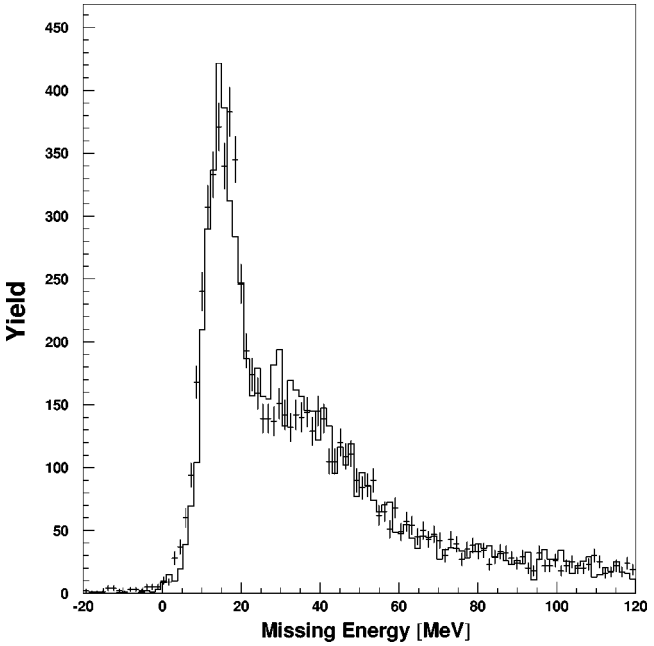

FIG. 2. Experimental yield (pluses) as a function of missing energy for the $^{12}C(e,e'p)$ reaction, with the hadron spectrometer positioned at the quasifree angle, compared to simulated yields (histogram), at $Q^2=6.1$ $(\mathrm{GeV}/c)^2$.

represent the results of the present measurement while the open symbols from a previous measurement [16] are shown for comparison. The solid line in the top panel represents the predictions for the Monte Carlo yield. The lower panel of

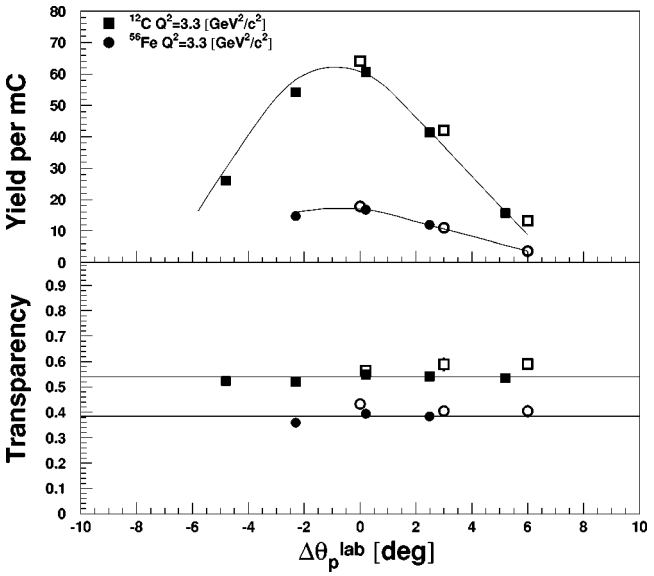

FIG. 3. (Upper panel) Experimental $(e,e'p)$ coincidence yields versus the difference between the proton spectrometer lab angle and the quasifree angle for data from $^{12}C(e,e'p)$ and $^{56}Fe(e,e'p)$ at $Q^2=3.3$ $(\mathrm{GeV}/c)^2$. Closed symbols are for the present experiment. Open symbols are for the data from Ref. [16]. (Lower panel) Transparency as function of proton angle for the same data. The curves in the top panel are simulations of the yield based on the model described in the text and normalized by a single transparency factor.

Fig. 3 shows the extracted transparency ratio for the ^{12}C and ^{56}Fe targets at the various angles measured. The solid line represents the statistically averaged transparency ratio from the present results and the result is seen to coincide with the central value within the errors of the measurement. Again the data (open symbols) from the previous measurement [16] are shown for comparison. The transparency ratio is also seen to be close to constant for the various angles about the quasifree angle. In the previous measurement [16] large asymmetries were seen in the ratios about the quasifree angle for $Q^2=0.8$ and 1.3 $(\mathrm{GeV}/c)^2$. This was interpreted as the presence of a longitudinal-transverse interference term in the measured cross section approximately 20% larger than what is contained in the off-shell σ_{ep} cross section. The disappearance of this asymmetry indicates that the reaction mechanism is simpler at these larger values of Q^2.

The nuclear transparencies for deuterium, carbon, and iron are given in Table II for the various Q^2 values measured. Typically, the point-to-point systematic uncertainty amounts to 2.3%, dominated by uncertainties in the beam current measurement (0.7%), run-to-run stability of (e,e') and (e,p) singles events ($<1\%$), and an estimated 1% for the proton absorption correction applied. The quoted 2.3% error does neither take into account a normalization-type uncertainty of 3%, nor the model-dependent systematic uncertainties implicit in the extraction of the transparency ratios. The normalization-type uncertainty is mainly due to the radiative corrections, the choice of electron-proton cross section, and knowledge of the spectrometers acceptance. The model-dependent uncertainties are target nucleus dependent and are due to choices in spectral function parameters and the uncertainty in correlation correction.

There are some exceptions to the 2.3% point-to-point systematic uncertainty. As mentioned previously, the deuterium transparency results were obtained by dividing by the corresponding measured hydrogen cross section data. This accounts for the normalization problems in the deuterium target due to the effects of the extended target. The results then were in good agreement with the earlier measurement [8,9]. Nonetheless, a larger systematic uncertainty of 3% was assigned to the deuterium results. The iron measurement at $Q^2=6.1$ $(\mathrm{GeV}/c)^2$ also was assigned a larger systematic uncertainty of 3.8%, because of uncertainty due to the target thickness.

III. *A* DEPENDENCE

The measured transparency $T(Q^2)$ values from this (large solid symbols) and previous work are presented in Fig. 4. The errors shown include statistical and systematic uncertainties, but do not include model-dependent systematic uncertainties in the spectral functions and correlation corrections used in the simulations. This is the same as for the data of Ref. [16] (small solid symbols). Data from previous experiments [8,9,27] (represented by open symbols) include the full uncertainty. For completeness, we also show results using gold targets, from previous experiments only. The present results for carbon and iron are of similarly high precision as those of Ref. [16], and of substantially higher pre-

TABLE II. Measured transparencies for D, C, and Fe. The first uncertainty quoted is statistical, the second systematic. In the figures these are added in quadrature. The uncertainties in the figures do not include model-dependent systematic uncertainties on the simulations. We note that a renormalization of these nuclear transparencies with a factor of 1.020 (T_C) and 0.896 (T_{Fe}) is advocated in Ref. [30].

Q^2 $(\mathrm{GeV}/c)^2$	T_D	T_C	T_{Fe}
3.3	$0.897 \pm 0.013 \pm 0.027$	$0.548 \pm 0.005 \pm 0.013$	$0.394 \pm 0.009 \pm 0.009$
6.1	$0.917 \pm 0.013 \pm 0.028$	$0.570 \pm 0.007 \pm 0.013$	$0.454 \pm 0.015 \pm 0.018$
8.1	$0.867 \pm 0.020 \pm 0.026$	$0.573 \pm 0.010 \pm 0.013$	$0.391 \pm 0.012 \pm 0.009$

cision than of Refs. [8,9,27]. Our results at $Q^2 = 3.3\ (\mathrm{GeV}/c)^2$ agree well with the previous results for deuterium [8,9], carbon, and iron [16].

Little or no Q^2 dependence can be seen in the nuclear transparency data above $Q^2 \approx 2\ (\mathrm{GeV}/c)^2$. Excellent constant-value fits can be obtained for the various transparency results above such Q^2. For deuterium, carbon, and iron, fit values are obtained of 0.904 (± 0.013) 0.570 (± 0.008), and 0.403 (± 0.008), with χ^2 per degree of freedom of 0.56,

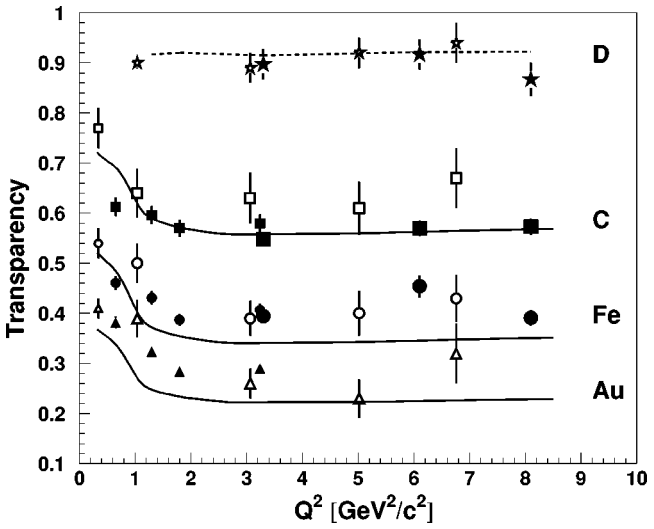

FIG. 4. Transparency for $(e,e'p)$ quasielastic scattering from D (stars), C (squares), Fe (circles), and Au (triangles). Data from the present work are the large solid stars, squares, and circles, respectively. Previous JLab data (small solid squares, circles, and triangles) are from Ref. [16]. Previous SLAC data (large open symbols) are from Refs. [8,9]. Previous Bates data (small open symbols) at the lowest Q^2 on C, Ni, and Ta targets, respectively, are from Ref. [27]. The errors shown for the current measurement and previous measurement [16] include statistical and the point-to-point systematic ($\pm 2.3\%$) uncertainties, but do not include model-dependent systematic uncertainties on the simulations or normalization-type errors. The net systematic errors, adding point-to-point, normalization-type and model-dependent errors in quadrature, are estimated to be ($\pm 3.8\%$), ($\pm 4.6\%$), and ($\pm 6.2\%$) corresponding to D, C, and Fe, respectively. The error bars for the other data sets [8,9,27] include their net systematic and statistical errors. The solid curves shown from $0.2 < Q^2 < 8.5\ (\mathrm{GeV}/c)^2$ are Glauber calculations from Ref. [28]. In the case of D, the dashed curve is a Glauber calculation from Ref. [29].

1.29, and 1.17, respectively. As in Ref. [16], we compare with the results from correlated Glauber calculations, including rescattering through third order [28], depicted as the solid curves for $0.2 < Q^2 < 8.5\ (\mathrm{GeV}/c)^2$. In the case of deuterium, we show (dashed curve) a generalized Eikonal approximation calculation, coinciding with a Glauber approximation for small missing momenta [29]. The Q^2 dependence of the nuclear transparencies is well described, but the transparencies are underpredicted for the heavier nuclei. This behavior persists even taking into account the model-dependent systematic uncertainties.

Recently, a new calculation of nuclear transparencies has become available [30]. This results in a better agreement between Glauber calculations and the A dependence of the nuclear transparency data. In this paper [30] it was argued that the uncertainty in the treatment of short-range correlations in the Glauber calculation can be constrained with inclusive $A(e,e')$ data. This results in an effective renormalization of the nuclear transparencies for the ^{12}C and ^{56}Fe nucleus of 1.020 and 0.896, respectively. Such a renormalization is due to integration of the denominator in Eq. (2) over a four-dimensional phase space V in E_m and $|\vec{p}_m|$ argued to be more consistent with experiments. That is, the experiment measures an angular distribution in the scattering plane rather than the complete $|\vec{p}_m| < 300$ MeV/c region. This reduces the influence of short-range correlations. The nuclear transparencies as given in Table II would have to be multiplied by these renormalization factors, rendering values more consistent with the A dependence of Glauber calculations. Although such a renormalization may be appropriate, we quote nuclear transparency numbers consistent with the procedure of Refs. [8,9,16], for the sake of comparison.

For the remainder of this section, we will concentrate on a combined analysis of the world's $A(e,e'p)$ nuclear transparency data. Figure 5 shows T as a function of A. The curves represent empirical fits of the form $T = cA^{\alpha(Q^2)}$, using the deuterium, carbon, and iron data. We find, within uncertainties, the constant c to be consistent with unity as expected and the constant α to exhibit no Q^2 dependence up to $Q^2 = 8.1\ (\mathrm{GeV}/c)^2$. A similar treatment to nuclear transparency results of the older $A(e,e'p)$ experiments renders a nearly constant value of $\alpha = -0.24$ for $Q^2 \geq 1.8\ (\mathrm{GeV}/c)^2$. Numerical values are presented in Table III. We note that using the renormalizations of the nuclear transparencies proposed by Frankfurt, Strikman, and Zhalov [30] would reduce the

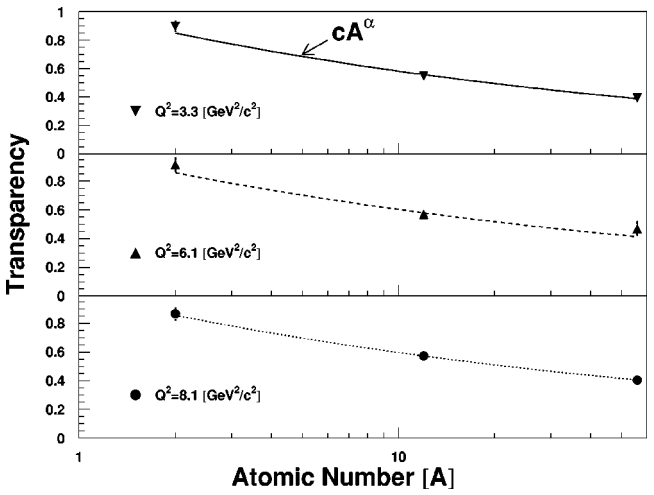

FIG. 5. Nuclear transparency as a function of A at $Q^2=3.3$, 6.1, and 8.1 $(\mathrm{GeV}/c)^2$ (top to bottom). The curves are fits to the D, C, and Fe data using $T=cA^{\alpha}$.

numerical values of α by ≈ 0.03.

Alternatively, we can analyze the T results from the different nuclei ($A \geqslant 12$), and the different experiments, in terms of a simple geometric model, similar to that used in Refs. [9,31]. This model assumes classical attenuation of protons propagating in the nucleus, with an effective proton-nucleon cross section σ_{eff} that is independent of density:

$$T_{\mathrm{class}}=\frac{1}{Z}\int d^3r\,\rho_Z(\mathbf{r})\exp\left[-\int dz'\,\sigma_{\mathrm{eff}}\rho_{A-1}(\mathbf{r}')\right]. \quad (3)$$

For this calculation, the nuclear (charge) density distributions were taken from Ref. [32] and σ_{eff} is the only free parameter. The difference in number of protons and neutrons for a heavy nucleus is taken into account in constructing σ_{eff}. It is possible that the effective change of σ_{pp} in a nuclear medium is different from that of σ_{pn}, but this is neglected.

TABLE III. Results of the fits to the A dependence (see text) using the world's data. Please note that the values quoted for σ_{eff} follow the framework of Ref. [31], and numerical values differ slightly from those quoted in Ref. [9].

Q^2 $(\mathrm{GeV}/c)^2$	Ref.	α	σ_{eff} (mb)
0.3	[27] (Bates)	-0.23 ± 0.03	17 ± 3
0.6	[16] (JLab)	-0.17 ± 0.04	24 ± 4
1.0	[8,9] (SLAC)	-0.18 ± 0.02	22 ± 3
1.3	[16] (JLab)	-0.22 ± 0.05	27 ± 3
1.8	[16] (JLab)	-0.24 ± 0.04	32 ± 3
3.1	[8,9] (SLAC)	-0.24 ± 0.02	30 ± 3
3.3	[16] (JLab)	-0.25 ± 0.04	30 ± 3
3.3	present work	-0.24 ± 0.02	35 ± 3
5.0	[8,9] (SLAC)	-0.24 ± 0.02	33 ± 4
6.1	present work	-0.24 ± 0.03	30 ± 4
6.8	[8,9] (SLAC)	-0.20 ± 0.02	24 ± 4
8.1	present work	-0.23 ± 0.02	33 ± 3

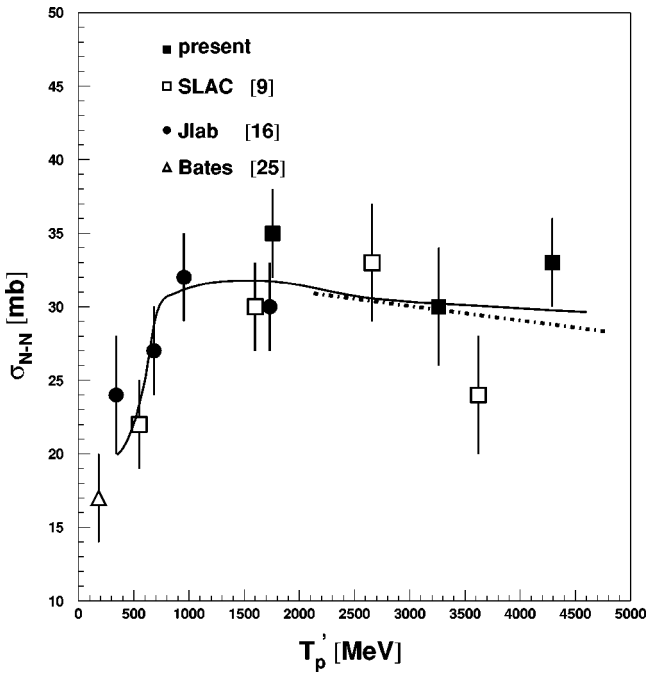

FIG. 6. Effective proton-nucleon cross section σ_{eff} as determined using a model assuming classical attenuation of protons propagating in the nucleus, with σ_{eff}, independent of density, as fit parameter (see text). The data are a compilation of the present work and previous work at JLab [16], SLAC [9], and Bates [27]. The solid curve is a fit to the effective nucleon-nucleon cross sections, assuming a similar energy dependence as the average of the free-proton–proton and proton-neutron cross sections from the Particle Data Booklet tables [33]. The dot-dashed curve, almost coinciding with the solid curve, is the result of a calculation of Ref. [36].

Finally, we also assume that the hard scattering rate is accurately determined by our PWIA model. Therefore, any energy dependence of the transparency is due to final-state interactions. Note that in the limit of complete CT, one would expect $\sigma_{\mathrm{eff}}\rightarrow 0$. The results of fitting this model to the measured T results are shown in Table III and Fig. 6. We also show, both in Table III and Fig. 6, the results of fits using the T values of Refs. [8,9,16,27]. Using the renormalization factors of the nuclear transparencies advocated by [30] results in values for σ_{eff} which are reduced by $\approx 2-3$ mb.

We compare, in Fig. 6, the results for σ_{eff} with a normalized parameterization of the free proton-nucleon scattering total cross sections [33] (solid curve). We observe no noticeable energy dependence of σ_{eff} beyond that of the free proton-nucleon scattering data. Thus, most of the variation of $T(A)$ as a function of Q^2 is a reflection of the energy dependence of the free N-N total cross section. In free-proton–nucleon scattering, the minimum at $T_{p'}\approx 500$ MeV is especially prominent [33], affecting the $T(A)$ values at $Q^2 \leqslant 1.3\ (\mathrm{GeV}/c)^2$.

Regarding the normalization, we find, with a χ^2 per degree of freedom of 0.9, an effective proton-nucleon cross section of $(71.4\pm2.4)\%$ of the free-proton–nucleon cross section. Such a reduction has been interpreted [9] as effectively taking into account effects such as Pauli blocking (at low energies) and short-range correlations, but is mainly an

artifact of the simple geometric model used in Eq. (3). For example, if one would fit, within the Glauber calculations of Ref. [34], an effective proton-nucleon cross sections to the present $^{12}C(e,e'p)$ nuclear transparency data, one would find far closer agreement with the free-proton–nucleon total cross sections. On an average, the reduction one finds in such a procedure is less than 10%.

Naively, the near constancy of the effective proton-nucleon cross section as function of Q^2, up to $Q^2 = 8.1$ $(\mathrm{GeV}/c)^2$, seems to rule out the onset of CT. However, the near constancy of transparencies versus Q^2, as shown in Fig. 4, may also result from a cancelling of effects in the hard electron-proton scattering and CT effects in the nucleon propagation [31]. One could argue that medium-dependent effects on hard electron-proton scattering will have a different A and Q^2 dependence than CT effects, but the geometric model used here is obviously too simple to incorporate a full description of the A dependence of the data.

If CT effects can be ruled out within the kinematics of the reported data, the near constancy of both the effective proton-nucleon cross section and the nuclear transparencies as function of Q^2 suggests that the quasi-free-electron–proton scattering cross section equals the free-electron–proton scattering cross section (corrected for off-shell effects as in Ref. [18]). If interpreted as constraining the medium modification of the proton magnetic form factor $G_M(Q^2)$, the T results for $Q^2 \geqslant 1.8$ $(\mathrm{GeV}/c)^2$ rule out a larger than 3% variation in the magnetic charge radius.

The typical effective proton-nucleon cross section found from this data analysis is ≈ 30 mb. This is much larger than that derived from the $A(p,2p)$ data of Ref. [4], translated to similar values of Q^2 or $T_{p'}$. Jain and Ralston [31] derive values of ≈ 15 mb from the latter data, using the same geometric model. It seems that a discrepancy exists, which is likely just related to both the validity of the simple geometric model used and the validity of the concept of an effective proton-nucleon cross section.

As mentioned earlier, the recent $A(p,2p)$ data [5] confirm the earlier trend in nuclear transparency. The data agree reasonably well with Glauber calculations [34] at incident beam momenta of 6 GeV/c and about 12 GeV/c, and show a rise and subsequent decrease in nuclear transparency in between. This rise and decrease seem consistent with the ratio of observed p-p cross section and the predicted hard scaling behavior. Thus, the nuclear filtering as proposed by Ralston and Pire [6] may be responsible for the apparent contradiction between the proton transparency results from $A(p,2p)$ and $A(e,e'p)$ results, in similar regions of Q^2. If so, it is not clear why the $A(p,2p)$ data numerically agree with Glauber calculations at incident beam momenta of 6 and 12 GeV/c, but not at 9 GeV/c. Alternatively, the apparent discrepancy may be related to the observation that the sensitivity to large momentum components in the nuclear wave function is different for $A(p,2p)$ and $A(e,e'p)$ [15]. Regardless, it seems that a Q^2 of 8 $(\mathrm{GeV}/c)^2$ is not sufficient yet to select small transverse size objects in the hard e-p scattering process.

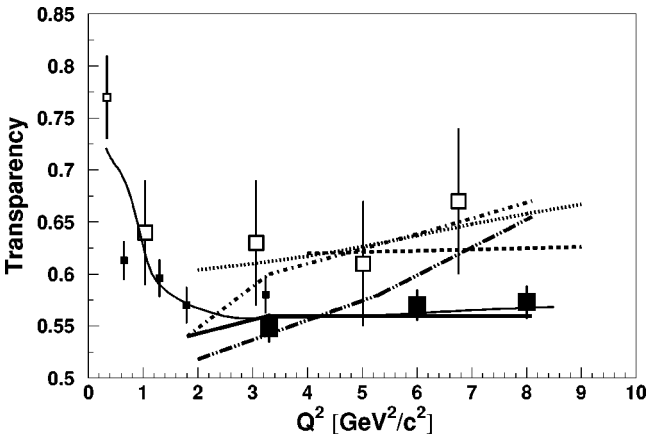

FIG. 7. Nuclear transparency for $^{12}C(e,e'p)$ quasielastic scattering. Symbols and thin solid curve are identical to Fig. 4. The errors shown include statistical and the point-to-point systematic ($\pm 2.3\%$) uncertainties, but do not include model-dependent systematic uncertainties on the simulations or normalization-type errors. The net systematic error, consisting of point-to-point, normalization-type, and model-dependent errors, is estimated to be ($\pm 4.6\%$). The error bars for the previous data sets [8,9,27] include their net systematic and statistical errors. The thick solid curve is a Glauber calculation of Ref. [34]. The dot-dashed, dotted, dashed, and dot-dot-dash curves are color transparency predictions from Refs. [34–36], and [37], respectively.

IV. Q^2 DEPENDENCE

The $^{12}C(e,e'p)$ reaction has important benefits for a detailed study of the onset of CT. The ^{12}C nucleus has a relatively simple nuclear structure, and the previous low-Q^2 measurements provide accurate information on its spectral function. Quasi-free-electron–proton scattering rates off ^{12}C nuclei are large due to the reduced transparency effects with respect to heavier target nuclei, which, although it reduces the sensitivity to CT effects, enables the use of statistics to perform studies of systematic uncertainties. In addition, a ^{12}C target can, unlike, e.g., an ^{56}Fe target, thermally withstand high (100 μA) electron beam currents. Thus, both the previous TJNAF experiment [16] and the present experiment obtained results of high precision in both statistics and systematics for nuclear transparencies determined from the $^{12}C(e,e'p)$ reaction. For these reasons, we used the $^{12}C(e,e'p)$ results to perform a statistical analysis of the Q^2 dependence of the nuclear transparency.

The $^{12}C(e,e'p)$ nuclear transparency results are shown in Fig. 7, with several calculations that do or do not include CT effects [28,34–37]. We note that there have been more calculations investigating CT effects in the $A(e,e'p)$ reaction [38–40]. However, these publications do not provide specific calculations for the $^{12}C(e,e'p)$ reaction, and will not be further discussed.

To reduce the influence of the energy dependence of the N-N total cross section, we restricted the analysis to energies substantially above the minimum in this cross section, i.e., to Q^2 values above 1.8 $(\mathrm{GeV}/c)^2$. Additionally, the normalizations of the various calculations were, in the statistical analysis, treated as a free parameter, as approximations concerning

e.g. the influence of short-range correlations and the density dependence of the N-N cross section will affect the absolute magnitude of the nuclear transparencies calculated (but have little influence on the Q^2 dependence for large enough Q^2). This enhances the sensitivity to a possible Q^2 dependence predicted by the inclusion of CT effects.

As in Fig. 4, the data are once more compared in Fig. 7 with the results of the correlated Glauber calculation of Ref. [28] (solid curve). In addition, various other calculations are shown. Kundu *et al.* [36] follow a perturbative QCD approach in the impulse approximation. Due to the hard scattering, only the short distance distribution amplitudes dominate. The ''expansion'' or diffusion in the quantum mechanical propagation of quarks sideways and longitudinally is included in the perturbative treatment. The effects of interaction with the nuclear medium is included through an Eikonal form. The calculation has to make an assumption on the distribution amplitudes. It appears [36] that perturbative QCD effects are better applied to the nuclear medium, due to suppression of long distance components, and that CT effects are slower for end-point-dominated (''double-bump'') distribution amplitudes, of, e.g., Refs. [41,42], rather than for the asymptotic (''single-bump'') distribution amplitude. In Fig. 7 a calculation with the distribution amplitude of Ref. [42] is shown (dashed curve). Furthermore, a calculation of the effective proton-nucleon cross section of Ref. [36], within the same framework, is added as a dot-dashed curve in Fig. 6, and is almost coinciding with our fit result. This may just reflect a similar neglect of detailed nuclear physics effects as in the simple geometric model of Eq. (3).

By contrast, Ref. [34] uses a more classical distorted-wave impulse approximation approach, starting from a realistic ansatz for the nuclear structure wave function and the optical limit to incorporate distortion effects. A quantum diffusion model is used to describe the expansion of the small size configuration selected in the (hard) scattering process to its physical size. The model depends on the hadronization length as a parameter, which in turn depends on the mass difference squared, ΔM^2, between the proton and the first inelastic diffractive intermediate state. The thick solid curve represents the correlated Glauber calculation of Ref. [34]. The dot-dashed curve represents the calculation with the inclusion of CT effects, under the assumption that $\Delta M^2 = 1.1\ \mathrm{GeV}^2$ [34].

Nikolaev *et al.* [35] assume that closure is allowed within the reasonably broad E_m and p_m acceptance of the nuclear transparency experiments, and calculate final-state interaction effects in the Glauber approximation. The calculation argues against an assumed factorization into a PWIA model and a global attenuation factor. CT effects, due to the interference of the elastic and inelastic intermediate states, are included based on an expansion of the struck nucleon wave function in terms of excited hadronic basis states. The dotted curve represents the result of this calculation. Jennings and Miller [37] also assume that the closure assumption is valid and comment that the matrix elements between the ground state nucleon and the first excited state N^* dominate the final-state interactions of the ejected system. In this calculation the mass M_1 of the first excited state dominates the rate of expansion of the small transverse size hadronic system. Evidently, lower-mass excited states yield a slower expansion rate allowing the hadronic system to escape the nucleus before evolving back to the normal hadron size. The dot-dot-dash curve is the result of their calculation with $M_1 = 1770$ MeV.

TABLE IV. Statistical comparisons of $^{12}\mathrm{C}(e,e'p)$ data with various model calculations. The first model is a Glauber calculation only, the alternative models incorporate color transparency effects. We also added entries assuming a floating normalization in these models, to take into account uncertainties both in assumptions made in the Glauber calculations and in the analysis.

Ref.	Normalization	χ^2/d.f.	Conf. level
[28] (Glauber)	Fixed	0.84	55%
[34] (Glauber)	Fixed	1.82	9%
[34] (+ CT)	Fixed	9.4	$<0.1\%$
	Floating	4.0	$<0.1\%$
[35] (+ CT)	Fixed	10.1	$<0.1\%$
	Floating	1.87	9%
[36] (+ CT)	Fixed	7.8	$<0.1\%$
	Floating	0.86	52%
[37] (+ CT)	Fixed	7.4	$<0.1\%$
	Floating	8.4	$<0.1\%$

Table IV displays the results of the statistical analysis, numerically showing the agreement between the data and various calculations in terms of the χ^2 per degrees of freedom and the confidence level of each calculation. The best descriptions are found for the correlated Glauber calculation of Ref. [28], and the calculation, including CT effects, of Ref. [36], assuming we allow for the mentioned floating normalization. The CT effects of the latter calculation imply only a 1% increase in nuclear transparency from $Q^2=4$ to 9 $(\mathrm{GeV}/c)^2$, assuming an end-point-dominated distribution. A fit to the existing world's data rule out any CT effects larger than 7% over the Q^2 range between 2.0 and 8.1 $(\mathrm{GeV}/c)^2$, with a confidence level of at least 90%, but are consistent with calculations incorporating CT effects of a few percent only, or no CT effects at all up to $Q^2 = 8.1\ (\mathrm{GeV}/c)^2$.

For the sake of completeness, we note that even a conclusive experimental observation of a rise in nuclear transparency, as a function of increasing Q^2, may not necessarily be an unambiguous observation of CT. Kopeliovich and Nemchik [38] argue that such a rise can also be caused by inelastic shadowing, due to the diffractive production of inelastic intermediate states by the knocked-out proton while it propagates through the medium.

V. CONCLUSIONS

Nuclear transparencies have been derived from a PWIA analysis of quasielastic $(e,e'p)$ scattering from deuterium, carbon, and iron nuclei up to $Q^2=8.1\ (\mathrm{GeV}/c)^2$.

The A and Q^2 dependence of these nuclear transparencies was investigated in a search for the onset of the CT phenomenon. The A dependence was parameterized as nuclear trans-

parency $T(Q^2)=cA^{\alpha(Q^2)}$. Using deuterium, carbon, and iron data we find, within uncertainties, the constant c to be unity as expected, and no Q^2 dependence of α, up to $Q^2=8.1$ $(\mathrm{GeV}/c)^2$. Alternatively, one can analyze the nuclear transparency data within a simple geometric model, using the effective proton-nucleon cross section as a free parameter [31]. We consistently find an effective proton-nucleon cross section with similar energy dependence as the free-proton–nucleon cross section. Thus, using the experimental energy dependence of the free-proton–nucleon cross section may be sufficient to describe the nuclear transparencies we measured in a detailed Glauber calculation.

In addition, we have performed a statistical analysis of the Q^2 dependence of the nuclear transparencies determined from the $^{12}\mathrm{C}(e,e'p)$ reaction, in comparison with state-of-the-art calculations with and without CT effects [28,34–36]. Combining the A- and Q^2-dependence analysis results, we find no evidence for the onset of CT within our range of Q^2.

ACKNOWLEDGMENTS

The authors would like to thank Dr. Jain, Dr. Ralston, and Dr. Strikman for disclosing results of their calculations prior to publication. This work was supported by grants of the United States Department of Energy and the National Science Foundation. The Southeastern Universities Research Association (SURA) operates the Thomas Jefferson National Accelerator Facility for the United States Department of Energy under Contract No. DE-AC05-84ER40150.

[1] A.H. Mueller, in *Proceedings of the Seventeenth Recontre de Moriond Conference on Elementary Particle Physics, Les Arcs, France, 1982*, edited by J. Tran Thanh Van (Editions Frontieres, Gif-sur-Yvette, France, 1982); S.J. Brodsky, in *Proceedings of the Thirteenth International Symposium on Multiparticle Dynamics, Volendam, The Netherlands, 1982*, edited by W. Kittel *et al.* (World Scientific, Singapore, 1983).
[2] D. Perkins, Philos. Mag. **46**, 1146 (1955).
[3] L.L. Frankfurt, G.A. Miller, and M.I. Strikman, Comments Nucl. Part. Phys. **21**, 1 (1992).
[4] A.S. Carroll *et al.*, Phys. Rev. Lett. **61**, 1698 (1988).
[5] Y. Mardor *et al.*, Phys. Rev. Lett. **81**, 5085 (1998); A. Leksanov *et al.*, *ibid.* **87**, 212301 (2001).
[6] J.P. Ralston and B. Pire, Phys. Rev. Lett. **61**, 1823 (1988).
[7] S.J. Brodsky and G.F. de Teramond, Phys. Rev. Lett. **60**, 1924 (1988).
[8] N.C.R. Makins *et al.*, Phys. Rev. Lett. **72**, 1986 (1994).
[9] T.G. O'Neill *et al.*, Phys. Lett. B **351**, 87 (1995).
[10] M.R. Adams *et al.*, Phys. Rev. Lett. **74**, 1525 (1995).
[11] M. Arneodo *et al.*, Nucl. Phys. **B429**, 503 (1994).
[12] K. Ackerstaff *et al.*, Phys. Rev. Lett. **82**, 3025 (1999).
[13] E.M. Aitala *et al.*, Phys. Rev. Lett. **86**, 4773 (2001).
[14] L.L. Frankfurt, G.A. Miller, and M.I. Strikman, Phys. Lett. B **304**, 1 (1993).
[15] G.R. Farrar, H. Liu, L.L. Frankfurt, and M.I. Strikman, Phys. Rev. Lett. **62**, 1095 (1989).
[16] D. Abbott *et al.*, Phys. Rev. Lett. **80**, 5072 (1998).
[17] P. Bosted, Phys. Rev. C **51**, 409 (1995).
[18] T. de Forest, Nucl. Phys. **A392**, 232 (1983).
[19] S. Frullani and J. Mougey, Adv. Nucl. Phys. **14**, 1 (1984).
[20] J.W. Negele, Phys. Rev. C **1**, 1260 (1970); J.W. Negele and D. Vautherin, *ibid.* **5**, 1472 (1972).
[21] J.W. Van Orden, W. Truex, and M.K. Banerjee, Phys. Rev. C **21**, 2628 (1980).
[22] X. Ji (private communication).
[23] L. Lapikás, G. van der Steenhoven, L. Frankfurt, M. Strikman, and M. Zhalov, Phys. Rev. C **61**, 064325 (2000).
[24] D. Dutta *et al.*, Phys. Rev. C **61**, 061602(R) (2000).
[25] D. Debruyne and J. Ryckebusch, Nucl. Phys. **A699**, 65 (2002).
[26] R. Ent, B.W. Filippone, N.C.R. Makins, R.G. Milner, T.G. O'Neill, and D.A. Wasson, Phys. Rev. C **64**, 054610 (2001).
[27] G. Garino *et al.*, Phys. Rev. C **45**, 780 (1992).
[28] H. Gao, V.R. Pandharipande, and S.C. Pieper (private communication); V.R. Pandharipande and S.C. Pieper, Phys. Rev. C **45**, 791 (1992).
[29] L.L. Frankfurt, W.R. Greenberg, G.A. Miller, M.M. Sargsian, and M.I. Strikman, Z. Phys. A **352**, 97 (1995); M. M. Sargsian (private communication).
[30] L. Frankfurt, M. Strikman, and M. Zhalov, Phys. Lett. B **503**, 73 (2001).
[31] P. Jain and J.P. Ralston, Phys. Rev. D **48**, 1104 (1993).
[32] H. De Vries, C.W. de Jager, and C. De Vries, At. Data Nucl. Data Tables **36**, 495 (1987).
[33] Particle Data Group, D. E. Groom *et al.*, Eur. Phys. J. C **15**, 1 (2000).
[34] L.L. Frankfurt, M.I. Strikman, and M.B. Zhalov, Phys. Rev. C **50**, 2189 (1994); M. Strikman and M. Zhalov (private communication).
[35] N.N. Nikolaev, A. Szczurek, J. Speth, J. Wambach, B.G. Zakharov, and V.R. Zoller, Phys. Rev. C **50**, R1296 (1994).
[36] B. Kundu, J. Samuelsson, P. Jain, and J.P. Ralston, Phys. Rev. D **62**, 113009 (2000); P. Jain and J.P. Ralston (private communication).
[37] B. Jennings and G. Miller, Phys. Rev. D **44**, 692 (1991).
[38] B. Kopeliovich and J. Nemchik, Phys. Lett. B **368**, 187 (1996).
[39] A. Kohama, K. Yazaki, and R. Seki, Nucl. Phys. **A551**, 687 (1993).
[40] O. Benhar, S. Fantoni, N. Nikolaev, J. Speth, A. Usmani, and B. Zakharov, J. Exp. Theor. Phys. **83**, 1063 (1996); Zh. Eksp. Teor. Fiz. **110**, 1933 (1996).
[41] V.L. Chernyak and A.R. Zitnisky, Nucl. Phys. **B246**, 52 (1984).
[42] I.D. King and C.T. Sachrajda, Nucl. Phys. **B279**, 785 (1987).